Nanoscale enzymatic compartments in tandem support cascade reactions in vitro

Journal:	*Biomacromolecules*
Manuscript ID	bm-2018-01019w.R1
Manuscript Type:	Article
Date Submitted by the Author:	31-Aug-2018
Complete List of Authors:	Belluati, Andrea; Universitat Basel, Departement Chemie Craciun, Ioana; Universitat Basel, Departement Chemie Liu, Juan; University of Basel Palivan, Cornelia; University of Basel, Chemistry Department

Nanoscale enzymatic compartments in tandem support cascade reactions *in vitro*

Andrea Belluati[1], *Ioana Craciun*[1], *Juan Liu*[1], *Cornelia G. Palivan*[1]*

[1]Department of Chemistry, University of Basel, Mattenstrasse 24a, CH-4058 Basel

KEYWORDS

Catalytic compartment, polymersome, cascade reaction, *in vitro*, gout

ABSTRACT

Compartmentalization at the nanoscale is fundamental in nature, where the spatial segregation of biochemical reactions within cells ensures optimal conditions for regulating metabolic pathways. Here, we present a nature inspired approach to engineer enzymatic cascade reactions taking place between separate vesicular nanocompartments (polymersomes), each containing one enzyme type. We propose by the selected combination of enzymes, an efficient solution to detoxify the harmful effect of uric acid and prevent the accumulation of the derived H_2O_2, both being associated with various pathological conditions (e.g. gout and oxidative stress). Fungal uricase and horseradish peroxidase combined to act in tandem, were separately encapsulated within nanocompartments, equipped with channel porins as gates to allow passage of substrates and products from each step of the reaction. We established the molecular factors affecting the efficiency of the overall reaction, and the protective role of the compartments. Interestingly, the

cascade reaction between separate nanocompartments was as efficient as for free enzymes in complex media, such as human serum. The nanocompartments were non-toxic towards cells and more importantly, addition of the tandem catalytic nanocompartments to cells exposed to uric acid provided simultaneous detoxification of uric acid and the H_2O_2. Such catalytic nanocompartments can be used as a platform for understanding fundamental factors affecting intra-cellular communication and introduce non-native metabolic reactions into living systems for therapeutic applications.

Introduction

In nature, various enzymatic reactions occur in confined environments where substrates are channeled in between enzymes, or signaling molecules are released and travel between compartments[1] serving to isolate reactive intermediates, concentrate substrates in a specific region or fine tune reaction pathways.[2] Inspired by nature, significant efforts have been made to confine enzymes within nanocompartments, such as protein cages, lipid/polymer based compartments and layer by layer capsules, resulting in enzymatic compartments.[1, 3-4] Enzymatic compartments are of particular interest as they offer a protective environment that increases the life-time of the encapsulated enzymes, essential for applications.[5-6] In this respect, a particularly appealing class of compartments are polymersomes generated by self-assembly of amphiphilic copolymers, as their membrane is more stable than the lipid membrane of liposomes, while maintaining biocompatibility if the chemical nature of the copolymer is appropriately selected.[7] A key aspect to allow the enzymatic reaction to take place *in situ,* inside the cavity of polymersomes, is to render their membrane permeable thus enabling an exchange of substrates

and products with their surroundings. Various approaches have been reported: i) using inherently porous polymersomes,[8-9] ii) using an external stimulus, such as pH, or by addition of a chemical agent to render the membrane permeable,[10-11] and iii) inserting biopores or membrane proteins in the membrane.[12-13]

Cascade reactions reported within nanocompartments mainly involve encapsulation of one type of enzyme and providing the second enzyme free in the surrounding medium.[6, 14] However, if one partner of the cascade reaction is free in solution it might be degraded, resulting in a decrease or even termination of the overall reaction. Co-encapsulating enzymes within the same nanocompartment solves this issue, but only a low co-encapsulation efficiency can be obtained due to the statistic process of formation of multi-enzyme-loaded polymersomes.[7]

A higher encapsulation efficiency of different enzymes can be achieved by linking the two enzymes together prior to encapsulation, using micrometer-sized compartments or the formation of compartments within compartments where small compartments and free enzymes are encapsulated inside micrometer-size compartments.[9, 15-18] Both binding the enzymes in one complex and the approach of compartments within compartments, which uses organic solvents and emulsions, have the disadvantage of hindering the catalytic activity of the enzymes thus decreasing the efficiency or blocking the reaction.

One approach, which allows for modularity while preserving the enzymes involved in the cascade reaction, is to design catalytic compartments working in tandem.[7] However, there are only very few examples of catalytic nanocompartments (CNCs) working in tandem[8, 10, 19-20] and, to the best of our knowledge, very few polymeric nanocompartments were evaluated in a more complex medium or *in vitro*.[21] In addition, the kinetics of the cascade reactions in separate compartments and the molecular factors affecting them were not investigated to determine

whether such CNCs still function in a more complex medium than buffers or to propose a therapeutically relevant solution.

Here, we present a bio-inspired approach to engineer CNCs working in tandem and propose, by an appropriate selection of the enzymes, an efficient solution to detoxify the harmful effect of uric acid and H_2O_2, associated with various pathologic conditions (e.g. gout and oxidative stress). Both gout and oxidative stress are known to induce severe health problems, associated with an increase in medical costs estimated to be above $6 billion per year in the US.[22] We used an amphiphilic block copolymer poly(2-methyloxazoline)-*block*-poly(dimethylsiloxane)-*block*-poly(2-methyloxazoline) ($PMOXA_6$-$PDMS_{44}$-$PMOXA_6$) for the formation of the nanocompartments,[23] and their membrane was rendered permeable by insertion of the bacterial porin Outer membrane protein F (OmpF).[24] The role of the polymersomes is to protect the encapsulated enzymes in order to prolong their stability, as a crucial step towards translational applications, as is intended by our selected enzymatic reaction. We selected as enzymes for the cascade reaction uricase (UOX) and horseradish peroxidase (HRP), which uses H_2O_2 produced by UOX, as the substrate to initiate the second reaction (Scheme 1).[25-27] This non-native combination of enzymes serves to sequentially decrease the concentration of uric acid and prevent the accumulation of H_2O_2, derived from the reaction of uric acid degradation, thus resulting in a dual therapeutic approach. While previous reports on cascade reactions between nanocompartments focused on the feasibility of model reactions,[20] here we go one step further to understand the molecular factors associated with the cascade reaction between separate compartments and to optimize their overall function. Next, we investigate their ability to function at increasing distances to mimic intra- and intercellular bio-distances as well as in human serum, prior to applying them to decrease uric acid and the accumulation of H_2O_2, from

the cellular milieu to advance their therapeutic application. Our approach opens the avenue to combine different enzymes inside separate nanocompartments to obtain complex, novel-to-nature enzymatic pathways with high potential in diagnostics and therapeutics.

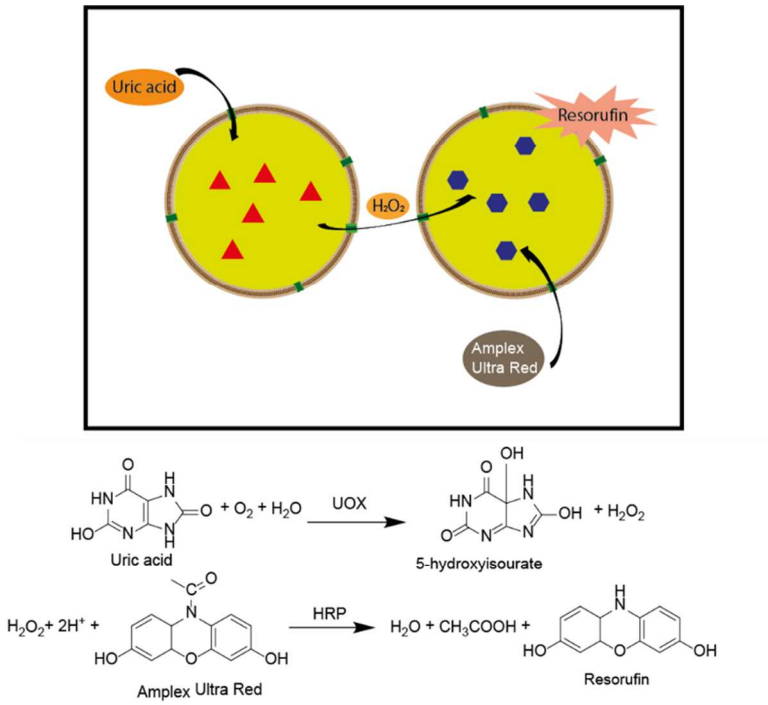

Scheme 1*. Schematic representation of catalytic nanocompartments (OmpF: green rectangle) working in tandem and detailed cascade reaction mediated by a combination of uricase (UOX, red triangles) and horseradish peroxidase (HRP, blue hexagons). The oxidation of uric acid results in formation of 5-hydroxyisourate and hydrogen peroxide. The latter is a co-substrate for HRP in presence of substrate Amplex Ultra Red, AR. The final product, resorufin, can be monitored by fluorescence spectroscopy.*

Materials

Dulbecco's Modified Eagle Medium with 4.5 g L^{-1} D-Glucose (DMEM-GlutaMax) was purchased from Gibco life technologies. Fetal calf serum (FCS) was purchased from BioConcept. CellTiter 96® Aqueous One Solution Cell Proliferation Assay (MTS) was purchased from Promega. The triblock copolymer $PMOXA_6$-$PDMS_{44}$-$PMOXA_6$ was kindly

provided by Prof. W. Meier, the University of Basel.[23] All other reagents and enzymes were purchased from Sigma-Aldrich unless otherwise specified.

Methods

OmpF expression and extraction

Wild-type OmpF was obtained according to a previously reported protocol,[28] with a few modifications: bacteria was grown at 30 °C for 6 hours on Terrific Broth (TB) (Difco, USA) and all ultracentrifugations were performed at room temperature (RT).

Preparation of catalytic nanocompartments

All CNCs were prepared at RT using the triblock copolymer $PMOXA_6$-$PDMS_{44}$-$PMOXA_6$ (obtained according to a previously reported procedure[23]) and wild-type OmpF, via the film rehydration technique. Films were rehydrated to a final polymer concentration of 4 mg mL^{-1} with 0.25 mg of UOX or HRP in PBS (pH 7) and 50 µl of previously dialyzed OmpF (60 µg mL^{-1} final concentration) or an equivalent volume of dialyzed octyl glucopyranoside, OG (Anatrace, USA) 3% for the non-permeabilized CNCs. Samples were extruded through an Avanti mini-extruder (Avanti Polar Lipids, USA) with a 200 nm pore diameter polycarbonate membrane (11 times). Non-encapsulated enzyme was removed through size exclusion chromatography (SEC) (Sepharose 4B column; 30 cm length).

Catalytic nanocompartment characterization — Static and Dynamic light scattering

Light scattering (LS) experiments were performed at 25 °C, using an ALV/CGS–8F goniometer (Langen/Hessen, Germany) equipped with a frequency-doubled He-Ne laser (LS instruments, λ

= 633). Static light scattering (SLS) was performed in 5° steps between 50° and 135° and analyzed with Zimm plot software (LS Instruments). Dynamic light scattering (DLS) was performed at 90° and analyzed through nonlinear decay-time analysis supported by cumulant fit.

Catalytic nanocompartment characterization — Transmission electron microscopy (TEM)

CNC suspensions in PBS at 0.25 mg mL^{-1} were deposited on glow-discharged carbon grids (Quantifoil, Germany) stained with 1.5% uranyl acetate solution and deposited on carbon-coated copper grids. A transmission electron microscope (Philips Morgagni 268D) at 293 K was used.

Catalytic nanocompartment characterization — Fluorescence correlation spectroscopy

Vesicles were labeled with BODIPY 630/650 SE (Thermo Fisher Scientific, USA) 100 nM.

All measurements were carried out using an LSM 880 confocal laser microscope (Carl Zeiss, Germany) with a 40x, 1.2 water immersion C-Apochromat objective lens. Measurements were performed at RT using a sample volume of 20 µL on a 22x50 mm glass slide. A HeNe laser at 633 nm was used for excitation of the BODIPY fluorophore, at 1% attenuation and pinhole 62 µm. The fluorescence signal was measured in real time and the autocorrelation function was calculated by the software calculator QuickFit 3.0.[29] Measurements were recorded over 5 s and each measurement was repeated 30 times. Experimental auto correlation curves were fitted using a two-component model including triplet state:

$$G(\tau) = 1 + \left(1 + \frac{T}{1-T} e^{-\frac{\tau}{\tau_{trip}}}\right) \frac{1}{N} \left(\frac{f_1}{1 + \frac{\tau}{\tau_{D1}} \sqrt{1 + R^2 \frac{\tau}{\tau_{D1}}}} + \frac{f_2}{1 + \frac{\tau}{\tau_{D2}} \sqrt{1 + R^2 \frac{\tau}{\tau_{D2}}}} \right)$$

f_1 and f_2 are respectively the fraction of the particles of the corresponding component 1 (dye) or 2 (vesicles), τ_{D1} represents the diffusion time of the dye and τ_{D2} the diffusion time of the vesicles, T

the fraction of fluorophores in triplet state with triplet time τ_{trip}, N is the number of particles and R the structural parameter, fixed at 5, according to the guidelines from Zeiss. The τ_{trip} and τ_D of free dye were determined independently, and subsequently fixed in the fitting procedure for dye-interacting vesicles. The confocal volume of 1 fL, was obtained by a calibration with free BODIPY and was necessary to determine the concentration of fluorescent particles (knowing the number of particles detected in the volume).

Enzyme quantification

The non-encapsulated enzyme fraction was recovered via SEC and the enhanced Pierce™ Bicinchonic Acid (BCA) assay was performed according to the supplier's protocol (Thermo Fisher Scientific, USA); instead of the BSA standards, both UOX (35 U mg^{-1}) and HRP (300 U mg^{-1}) calibration curves were prepared for the quantification of the respective samples. The amount of un-encapsulated protein was multiplied by the volume recovered from the column and then subtracted from the amount initially added to the rehydration solution, yielding the total amount of enzymes within the vesicles, divided by the volume of the vesicle (first fraction), *i.e.* the final concentration of the protein. This was performed on samples with no inserted OmpF, because the presence of the hydrophobic porin is not expected to influence the encapsulation efficiency of hydrophilic enzymes. The number of enzyme molecules was then divided by the number of vesicles, obtaining the number of enzymes per vesicle.

Enzyme activity and kinetics

Kinetic parameters were calculated using the Michaelis-Menten model:

$$v = \frac{V_{max}[S]_0}{K_M + [S]_0}$$

$$k_{cat} = \frac{V_{max}}{[E]_0}$$

Where v is the velocity of the enzyme, V_{max} is the maximum velocity at saturating concentration, $[S]_0$ is initial the concentration of the substrate S, K_M is the Michaelis-Menten constant. k_{cat} is the turnover number, the number of chemical conversions per second, $[E]_0$ is the concentration of catalytic sites (both for UOX and HRP it is equivalent with the concentration of enzyme).

In all experiments involving a cascade reaction, UOX was added in excess to HRP, to partially compensate for the former enzyme's lower activity, so that the ratio between production (from UOX, 35 U mg^{-1}) and consumption (from HRP, 350 U mg^{-1}) of hydrogen peroxide would not be the limiting factor. All enzymatic measurements were performed using a Spectramax M5 microplate reader (Molecular Devices, USA), in a in a 96-well, flat bottomed UV-transparent plate (Corning, USA) for uric acid absorbance (290 nm) or in a black plate (Thermo Fisher Scientific) for resorufin fluorescence (excitation 570 nm / emission 595 nm). The final volume in each well was of 200 µL in PBS. UOX concentration was increased ten-fold in cascade reaction experiments, to counter the slower native activity per weight of the enzyme, compared to the downstream enzyme HRP. Both uric acid consumption and resorufin production were quantified by means of calibration curves ($R^2 > 0.9$ for both curves). Each experiment was performed in triplicate and data was collected over 15 minutes (10 for the measurement of kinetic parameters).

UOX kinetics

UOX or UOX-loaded CNCs (final concentration of 3 µg mL^{-1}) were incubated in presence of increasing concentrations of the substrate uric acid (25, 100, 200, 400 and 800 µM) and the initial velocity of the enzymatic reaction was determined. The consumption of uric acid was

monitored and the data fitted with Graphpad Prism 7 software, obtaining K_M, V_{max} and k_{cat} values.

HRP kinetics

HRP or HRP-loaded CNCs (final concentration of 3 μg mL^{-1}) were incubated in the presence of 10 μM H_2O_2 and increasing concentrations of Amplex Ultra Red (AR) (Invitrogen) ranging from 0.2 to 20 μM. The initial velocity of the enzymatic reaction was determined by monitoring the formation of resorufin. The data was fitted using Graphpad Prism 7 software, obtaining K_M, V_{max} and k_{cat} values.

UOX-HRP cascade kinetics

Both reactions were examined when in a cascade: UOX or UOX-loaded CNCs (final concentration of 3 μg mL^{-1}) were added to HRP or HRP-loaded CNCs (final concentration 300 ng mL^{-1}) and both uric acid and AR were alternatively varied according to the previously listed concentrations.

Amplex Ultra Red conversion assay in a cascade

The same cascade reaction was tested at different conditions: UOX or UOX-loaded CNCs (final concentration of 3 μg mL^{-1}) were added to HRP or HRP-loaded CNCs (final concentration 300 ng mL^{-1}), uric acid to a final concentration of 10 μM and AR to a final concentration of 1 μM, unless in controls where either substrate was missing and was substituted by the same volume of PBS. The reaction profile in presence of catalase (1000 U mg^{-1}, final concentration of 10 μg mL^{-}

[1]) was blanked against the reaction profile of catalase alone in presence of AR, as catalase too has a heme center capable of reacting with the fluorogenic molecule.

Catalytic nanocompartment resilience to degrading agents

Concentrations were 3 μg mL^{-1} for UOX or UOX-CNC and 300 ng mL^{-1} for HRP or HRP-CNC. For the heat resistance assay, aliquots of the polymersome were incubated at 37, 50, 60 and 75 °C for either 10 or 30 minutes. For the chemical and enzymatic resistance assays, aliquots were incubated with 6 M guanidine hydrochloride (GdnHCl) for 1 hour and 0.1 mg ml^{-1} Proteinase K for 2 hours (37 °C), respectively. Proteinase K was added in excess with respect to the other enzymes (free and encapsulated). The production of resorufin was compared to that of the cascade reaction with no additional elements and the ratio was calculated. To verify unspecific binding, the same amount of enzyme (either UOX or HRP) was added to pre-formed empty vesicles and then purified with the same protocol, then mixed with vesicles encapsulating the other enzyme and the cascade kinetics were followed.

Activity of CNCs in serum

Activity in biological fluid was tested in human blood serum in which uric acid was dissolved to a final concentration of 500 μM at 37 °C, mimicking hyperuricemia. UOX or UOX-CNCs were added to reach a final concentration of 18 μg ml^{-1}, HRP or HRP-CNCs to 900 ng ml^{-1}, AR to 10 μM. The decrease of absorbance at 290 nm was monitored over the course of 6 hours. The degradation of uric acid was defined as

$$Relative\ urate\ degradation = \frac{\frac{\Delta Abs290_{with\ enzyme}}{min}}{\frac{\Delta Abs290_{no\ enzyme}}{min}},$$

Dependence of distance over reaction efficiency

Knowing the amount of CNCs in a given volume (obtained from FCS measurements), it was possible to calculate the mean inter-vesicle distance, assuming a cubic space occupied by the compartments, as

$$\frac{1}{\sqrt[3]{\frac{N}{V}}}$$

where N is the number of particles (sum of UOX and HRP loaded-polymersomes) and V is the reaction volume. A constant concentration of UOX-CNCs was mixed with a solution of HRP-CNCs at concentrations: 2x, 1x, 0.5x, 0.25x, 0.1x, 0.02x, 0.01x and 0.005x. The decrease in concentration of HRP-CNCs induced an increase of the mean distance between polymersomes, which was calculated using $N = N_{UOX\text{-}CNC} + N_{HRP\text{-}CNC}$. Resorufin production was monitored as described above.

Cell culture

HEK293T cells were cultured in a humidified atmosphere with 5% CO_2 at 37 ^{o}C in Dulbecco's Modified Eagle Medium with GlutaMAX^{TM}-I (4.5 g L^{-1} D-Glucose, Gibco life technologies) and supplemented with 10% Fetal calf serum (FCS, BioConcept), 100 U mL^{-1} penicillin and 100 µg mL^{-1} streptomycin (Sigma Aldrich).

Cell viability assay-MTS

For cell viability assessment, a CellTiter 96® Aqueous One Solution Cell Proliferation Assay (MTS, Promega) was used according to manufacturer instructions. Cells were seeded (5 000 cells/well in 100 µL cell culture medium) in a 96-well plate and incubated for 24 h. After 24 h

the UOX-HRP-CNCs (concentrations ranging from 1.18 to 18 μg mL^{-1} of total polymer) were diluted in PBS and added to the cells to reach a final volume of 200 μ/well. After 24 h incubation in presence of the CNCs, 20 μL MTS reagent was added to each well. After 4 h absorbance was measured at 490 nm using a Spectramax M5e plate reader. Background absorbance from control wells containing all assay components without cells was subtracted from each well and data normalized to control cells containing all components except CNCs.

Cell viability in presence of uric acid

Cells were seeded at a density of 5 000 cells/well in 100 μL cell culture medium, in a 96-well plate and incubated for 24 h. Next, cells were dosed with 250 or 500 μM of uric acid, final concentration, in the presence or absence of UOX-HRP-CNCs (18 μg mL^{-1} for UOX and 0.9 μg mL^{-1} for HRP, final concentrations in 200 μL final volume) or in the presence of free enzymes (UOX and HRP) at the same concentration. AR (1 μM, final concentration in 200 μL final volume) was added to each well as a co-substrate for the HRP-CNCs. After a 24 h incubation period, 20 μL MTS reagent was added to each well. The absorbance was measured at 490 nm after 4 h. Background absorbance from control wells containing all assay components apart from the cells was subtracted from each well and data normalized to control cells containing all components except CNCs and uric acid.

Statistics

Multiple t-tests were performed using Graphpad Prism 7 software, comparing datasets, without assuming constant standard deviation (SD). Statistical significance ($p<0.05$) was corrected using

the Holm-Sidak method. Significance was marked as * $p < 0.05$, ** $p < 0.01$, *** $p < 0.001$, sample size was always n = 3.

Results and Discussion

Formation of UOX-Catalytic nanocompartments and HRP-Catalytic nanocompartments

We encapsulated UOX and HRP inside the supramolecular assemblies formed during the self-assembly process of the copolymer by using film rehydration method due to its mild conditions, which do not affect the biomolecules.[7, 30] The architecture of the supramolecular assemblies in presence and absence of enzymes was established by a combination of LS and TEM. We used SLS to obtain the radius of gyration R_g, and DLS for the hydrodynamic radius R_h. The ratio of these values R_g/R_h, called ρ-factor, is indicative of the different architectures, e.g. 1 for hollow spheres while 0.77 for solid spheres.[31] In the case of empty supramolecular assemblies, R_g and R_h values were 70 ± 33 nm and 84 ± 25 nm respectively, and the calculated ρ-factor of 0.96 indicates hollow sphere architecture, thus formation of polymersomes. In the presence of UOX (UOX-CNC), we determined for the supramolecular assemblies an R_g of 68 ± 12 nm and R_h of 73 ± 33 nm (ρ = 0.95), while in the presence of HRP (HRP-CNC) they had an R_g of 74 ± 35 nm and R_h 85 ± 41 nm (ρ = 0.87) (Figure S1). In both cases, the enzymes did not affect the self-assembly process and resulted in polymersome architecture, which agrees with the TEM micrographs (Figure 1A and 1C, Figure S2 and S3).

In order to quantify the amount of encapsulated enzymes inside the nanocompartments, we used a combination of brightness measurements in FCS and BCA. FCS measures the fluorescence fluctuations due to the Brownian motion of fluorescent species in a fL-sized volume, yielding molecular parameters such as diffusion time and the number of particles that can be used to

evaluate interactions/encapsulation of the fluorescent dyes with/in supramolecular assemblies.[32] By labeling the vesicle membrane with BODIPY 630/650, and using a 2-component fit (fixing the diffusion time of free dye as one of the components) we obtained their average diffusion time (τ_D 5000 μs for both CNCs, as compared to τ_D = 57 μs of the free dye) and overall number of fluorescent vesicles in solution. The fraction of dye-polymersomes was 99% for UOX-CNCs and 94% for HRP-CNCs (2.6×10^{11} and 3.9×10^{11} polymersomes μL^{-1}, respectively), while that of the free dye 1% and 4% thus indicating that most of the dye partitioned into the polymersome membrane (Figure 1B and 1D).

A total protein concentration of 30 μg mL^{-1} for UOX and 18.6 μg mL^{-1} for HRP, was obtained by BCA assay (Figure S4). Dividing the protein concentration by the number of polymersomes obtained by brightness measurements, we determined an average of 11 ± 7 enzymes in UOX-CNCs and 6 ± 2 enzymes in HRP-CNCs. An encapsulation efficiency of 36 ± 12 % for UOX and 22 ± 4% for HRP inside CNCs was obtained, in agreement with the encapsulation efficiency values obtained for other enzymes inside polymersomes.[7, 30] A number of 11 OmpF/polymersome was inserted as we used similar conditions as previously reported.[33] We kept the amount of porin constant in order to distinguish the effect of all other molecular factors on the cascade reaction.

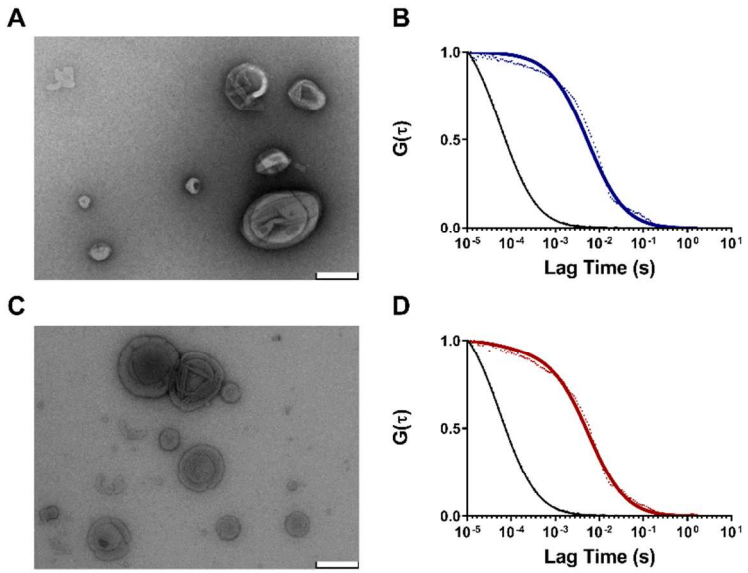

Figure 1. *Formation of UOX-CNCs and HRP-CNCs.* ***A:*** *TEM micrograph of UOX-CNCs (scale bar: 200 nm).* ***B****: normalized FCS autocorrelation curve of the dye labeled UOX-CNCs (dots: normalized raw data; solid line: fitted data, black line: free BODIPY 630/650).* ***C****: TEM micrograph of HRP-CNCs (scale bar: 200 nm).* ***D****: normalized FCS autocorrelation curve of the dye-labeled HRP-CNCs (dots: normalized raw data; solid line: fitted data, black line: free BODIPY).*

Overall enzymatic efficiency of CNCs

Having determined the amounts of encapsulated enzymes, we used the same concentrations in bulk to evaluate the efficiency of the cascade reaction. The cascade reaction takes place when the enzymes are free or encapsulated in separate nanocompartments equipped with OmpF (Figure 2A). The reaction cannot proceed when the membrane of the nanocompartments is not equipped with OmpF, to allow molecular passage through (Figure 2B), or when one of the enzymes or substrates is removed from the cascade (Figure 2C).

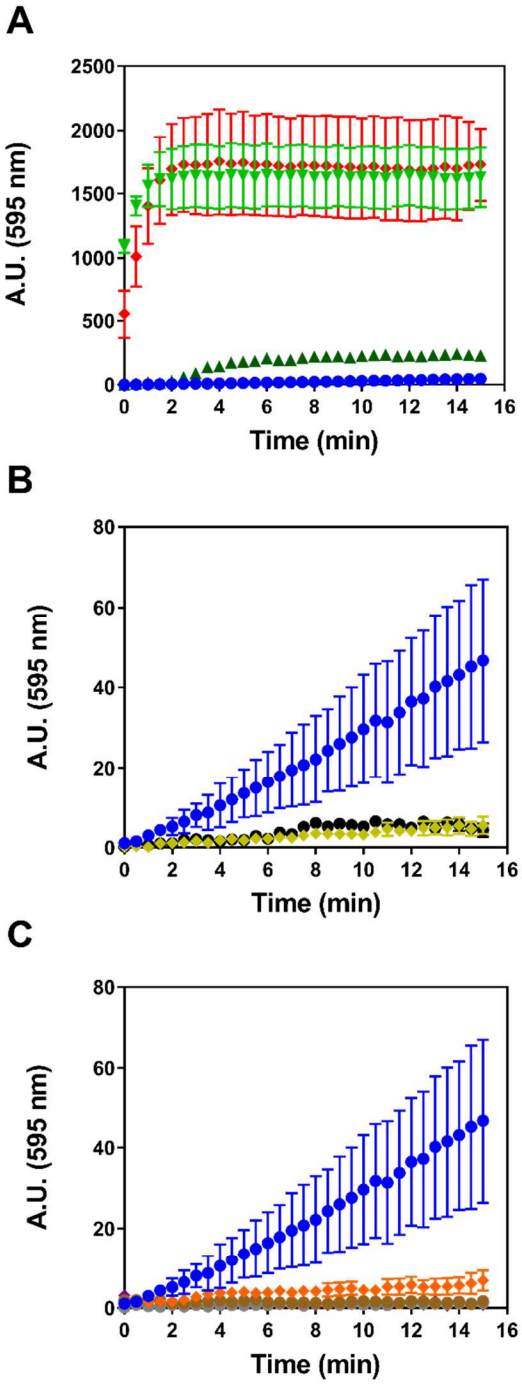

Figure 2. *Cascade reaction with different setups.* ***A****: Enzyme kinetics when both enzymes are free (red), only HRP is free (light green), only UOX is free (dark green) and both UOX and HRP are encapsulated inside polymersomes (blue).* ***B****: Cascade with permeabilized CNCs (blue), unpermeabilized UOX-loaded polymersomes (olive), unpermeabilized HRP-loaded polymersomes (black).* ***C****: Cascade reaction with both CNCs and the corresponding substrates (blue), and in the absence of one of the reaction*

compounds: HRP (orange), UOX (brown), AR (grey), and uric acid (purple). Error bars are given as mean ± SD (n = 3), in some cases bars are smaller than the corresponding dot.

As expected, the cascade reaction between separate nanocompartments is significantly slower than that of the free enzymes. Going a step further, we were interested in establishing the effect of the molecular diffusion through OmpF of substrates and products, examining the probability that the product of the first reaction penetrates in a second CNC containing the HRP and studying the effect of the distance between different CNCs on each step of the reaction and on its overall efficiency. The conversion of AR to resorufin (AR conversion) was used as a comparison standard, because it represents the last step of the cascade reaction and therefore accounts for whether the whole cascade reaction takes place. First, we studied the influence of molecular diffusion through OmpF as a key factor, which might limit the *in situ* enzymatic reaction inside CNCs. Having one of the enzymes free in solution and the second one encapsulated in the CNCs, AR conversion decreased compared with that of free enzymes. When HRP was surrounding UOX-CNCs, a slight decrease in AR conversion to 92% was observed, while when UOX was free around the HRP-CNCs, a significant decrease in AR conversion to 13% was obtained (Figure 3). When both enzymes were encapsulated within the CNCs working in tandem, AR conversion decreased significantly to 3% after 15 minutes. As H_2O_2 is known to rapidly diffuse through OmpF and it passes through the same barriers (membrane and inter-vesicle space) regardless of which enzyme is inside the CNCs, its effect is only minor and is due to its probability to interact with HRP. When only UOX is inside the CNCs, the slight decrease in AR conversion is due to an inhomogeneous distribution of UOX-CNCs, which are the only source of H_2O_2. When HRP is inside the CNCs, the greater decrease in AR conversion is related to the slow diffusion of AR through the OmpF pores, which is also the bottleneck for the cascade

reaction between CNCs in tandem. Another factor that contributes to the significant decrease in the reaction efficiency when CNCs are in tandem is the inhomogeneous CNC distribution which reduces the probability that the substrates of the second reaction reach the HRP-CNCs. Besides, the necessity of H_2O_2 transfer from UOX-CNCs to HRP-CNCs is proven by introducing free catalase to the reaction mixture, as a competing enzyme that converts H_2O_2 to water and oxygen (without Amplex Red as co-factor): when added, catalase strongly hinders the reaction mediated by HRP (Figure S5A).

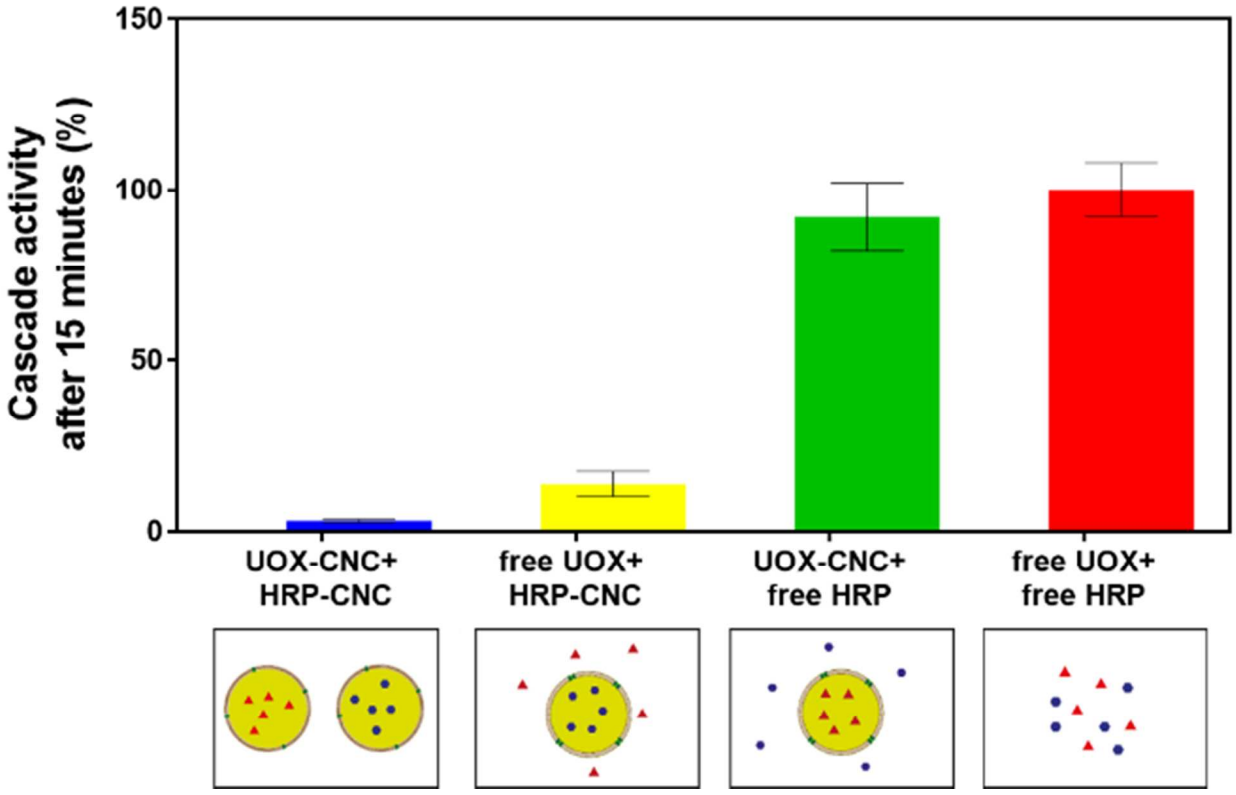

***Figure 3**. Conversion of AR to resorufin by a cascade enzymatic reaction when: both enzymes are encapsulated (blue), and only HRP is encapsulated (HRP-CNCs) and UOX is free (yellow), only UOX is encapsulated (UOX-CNCs) and HRP is free (green), both enzymes are free (red). Error bars are given as mean ± SD (n = 3).*

Kinetic analysis of CNCs

It is already known that encapsulation in polymersomes affects the kinetic parameters of enzymes, by increasing their affinity for the substrates or decreasing the velocity, because they are in a different environment than in solution.[30] To characterize the behavior of CNCs, we first compared the kinetic parameters of CNCs when isolated and then when acting in tandem by using the Michaelis-Menten model (Table 1 and 2, Figure S6). Both steps of the cascade reaction can be modeled in a first approximation by using Michaelis-Menten kinetics because in the first reaction (UOX-CNCs) uric acid is added in excess, and for the second step both substrates are in excess in the surroundings of the HRP-CNCs (AR added in excess in the medium, and H_2O_2 generated by UOX-CNCs with V_{max} of $1.47x10^{-3}$ μM/min, which is one order of magnitude higher than V_{max} of HRP, as presented in Table 1 and 2).

K_M, the Michaelis-Menten constant, defines the affinity of the enzyme for the substrate, and the apparent V_{max} represents the maximal velocity at which the enzyme operates once it is saturated by the substrate. As both K_M and V_{max} are intrinsic characteristics of the enzymes in specific conditions, it is expected that these parameters are not affected by the enzyme encapsulation (if the substrate/products diffusion is not changing due to possible barriers). However, we observe a completely different situation: both K_M and V_{max} are affected by enzyme encapsulation (Table 1 and 2).

The apparent K_M of both enzymes is lowered once confined in the nanocompartment, 4-times for UOX-CNC and 1.5 times for HRP-CNC, which is in agreement with a previous publication where encapsulated enzymes tend to exhibit a lowering in K_M.[34] However, this is not surprising as the hollow cavity of a polymersome offers a more confined space, increasing the probability of the substrate to access the catalytic center of the enzyme.[30] In addition, there is a decrease in

V_{max} and k_{cat} values. The decrease of both V_{max} and k_{cat} is significant in the case when UOX is encapsulated in the CNCs (both for free HRP and for HRP-CNCs) (Table 1). On the contrary, when HRP is encapsulated (free UOX and UOX-CNCs), the decrease in V_{max} and k_{cat} values is noticeably smaller (Table 2). We assume the change in k_{cat} values is associated with a slower influx of the substrates to the enzyme's active site, a slower efflux of the products or a combination thereof when the enzymes are inside the CNCs due to various barriers associated with the polymersomes architecture. Similarly, k_{cat} /K_M values decrease when the enzymes are inside the CNCs. While the substrate can easily encounter the enzyme once inside the compartment, the permeation through the membrane that is mediated by OmpF pores effectively hinders the total activity of the cascade. The effect of diffusion to the enzyme is a well-known parameter affecting and altering enzyme kinetics, as it can become the actual limiting factor in their efficiency.[35-36]

Table 1. *Apparent kinetic parameters for UOX: Michaelis-Menten constant (K_M), maximal enzyme velocity (V_{max}), turnover rate (k_{cat}) and catalytic efficiency (k_{cat}/K_M).*

	Free UOX	**Free UOX in cascade**	**UOX-CNC**	**UOX-CNC in cascade**
K_M (μM)	3.70×10^{2}	3.68×10^{2}	8.32×10^{1}	9.09×10^{1}
V_{max} (μM/min)	2.47×10^{-1}	2.77×10^{-1}	1.22×10^{-4}	1.47×10^{-3}
k_{cat} (1/s)	2.72	2.55	1.34×10^{-3}	2.00×10^{-3}
k_{cat} /K_M (1/(μM s))	7.30×10^{-3}	7.52×10^{-3}	1.60×10^{-5}	2.20×10^{-5}

***Table 2**. Apparent kinetic parameters for UOX: Michaelis-Menten constant (K_M), maximal enzyme velocity (V_{max}), turnover rate (k_{cat}) and catalytic efficiency (k_{cat}/K_M).*

	Free HRP	**Free HRP in cascade**	**HRP-CNC**	**HRP-CNC in cascade**
K_M (μM)	3.50×10	3.0×10	2.22×10	1.92×10
V_{max} (μM/min)	7.82×10^{-4}	8.19×10^{-4}	4.21×10^{-5}	1.32×10^{-4}
k_{cat} (1/s)	1.14×10^{-2}	1.12×10^{-2}	1.94×10^{-3}	6.19×10^{-3}
k_{cat}/K_M (1/M/s)	4.10×10^{-4}	4×10^{-4}	2.80×10^{-4}	3.22×10^{-4}

We exclude that the decrease in enzyme activity inside the CNCs is due to the confinement of enzymes: encapsulated UOX (molecular radius 4.27 nm[37]) and HRP (molecular radius 2.98 nm[38]) move free in a 1000-fold and 12000-fold greater volume inside the polymersome than their intrinsic volume, respectively. We calculated the inner volume of polymersomes as the volume of a sphere with a radius $R = R_h - d$, where d is the polymersome membrane thickness of 10.7 nm (previously determined for $PMOXA_6$-$PDMS_{44}$-$PMOXA_6$ compartments[39]).

Role of compartmentalization on CNC activity

In a similar manner as is the case for liposomes, the polymeric membrane of nanocompartments is expected to offer protection of the encapsulated payload from external agents that would degrade it, as for example proteolytic attack.[40] We wanted to establish the protective role of the

nanocompartments in the presence of physical factors such as high temperatures and different pH values as well as degrading agents (GdnHCl and Proteinase K). We quantified the "activity retention" as the ratio between the production of resorufin under standard conditions (RT, pH 7) and in the presence of degrading conditions. Wild-type OmpF is known to be stable at relatively extreme pH,[41-43] resistant to proteolysis,[44] chaotropic agents and temperatures up to 75 °C.[43] Therefore, the porin is neither affected by the mild conditions of the rehydration method used to generate the catalytic compartments, nor by the presence of a more complex environment or degrading agents, because it is also protected inside the compartments membrane.

While below 37°C both encapsulated and free enzymes preserve their activity, for higher temperatures, a decrease in activity is observed, but to a significantly higher degree for the free enzymes (Figure 4A, Figure S5D and S7). The ability of the polymeric membrane to protect the encapsulated payload from the effect of higher temperatures,[45-46] which denatures the enzymes, is essential for translational applications. The effect of pH was less straight forward, as these two enzymes have a different pH optima: basic for UOX and acidic for HRP.[47-48] While at pH 3 there is no apparent gain in activity from the enzyme encapsulation, at pH 9 the CNCs are significantly more active than the free enzymes acting in tandem (Figure 4B). The enzyme activity is further affected upon encapsulation due to a complex scenario: i) the interplay between the lower stability of HRP at higher pH values[49] and the basic pH optimum of UOX, ii) the stabilization of HRP –known to interact with hydrophobic substrates[50]– once inside the compartment, and iii) an increase in enzyme accessibility for the substrates due to the confined reaction space.[30] Therefore the effect of the pH on activity is less evident when the enzymes are free in solution and no confinement effects are present. However, we chose a neutral pH to evaluate the CNCs in tandem to be closer to physiological conditions, at which both enzymes are still active (Figure

S5B), and where both the free enzymes and encapsulated ones have similar activity retention values.

The addition of an enzyme denaturing chemical agent, such as GdnHCl, decreased the enzyme activity, which is significantly more pronounced when the enzymes are free. This clearly indicates the protective role of compartmentalization (Figure 4C). The decrease in activity retention values in the case of CNCs in tandem is mainly due to the diffusion of GdnHCl (95 Da) through OmpF, which has a weight cut-off of 650 Da.[51] Even though in a previous report GdnHCl diffused through the polymersome membrane,[52] this is not observed here as shown by the highly retained activity. The permeability of PMOXA-PDMS-PMOXA membranes varies depending on the molecular factors, such as the thickness of the membrane, the polydispersity of the copolymer chains or the conditions in which they are formed. In addition to the small number of inserted OmpF that are enough to allow *in situ* enzymatic reaction, the innate resistance towards denaturation of UOX [53-54] and the possible stabilization of HRP due to interactions with the membrane are responsible for maintaining enzymes' activity in the case of our CNCs, even in presence of GdnHCl.

To mimic a proteolytic attack, we added Proteinase K both to free enzymes and the CNCs for 2 hours. While a significant decrease in activity retention was observed for the free enzymes (18 ± 1%), in the case of CNCs the decrease was considerably smaller (83 ± 3%), additionally showing that a small fraction of enzyme molecules was adsorbed at the outer interface of the polymersome[33] (Figure 4D). We considered the overall activity of the CNCs as a whole; however, by adding free enzymes to empty vesicles and then purifying them, it was possible to detect a certain amount of activity due to unspecific binding in the cascade for HRP, estimated to

be around 3% of the total (Figure S5C and Table S1). The auto-oxidation of AR was also taken into account, and subtracted in all blanks.

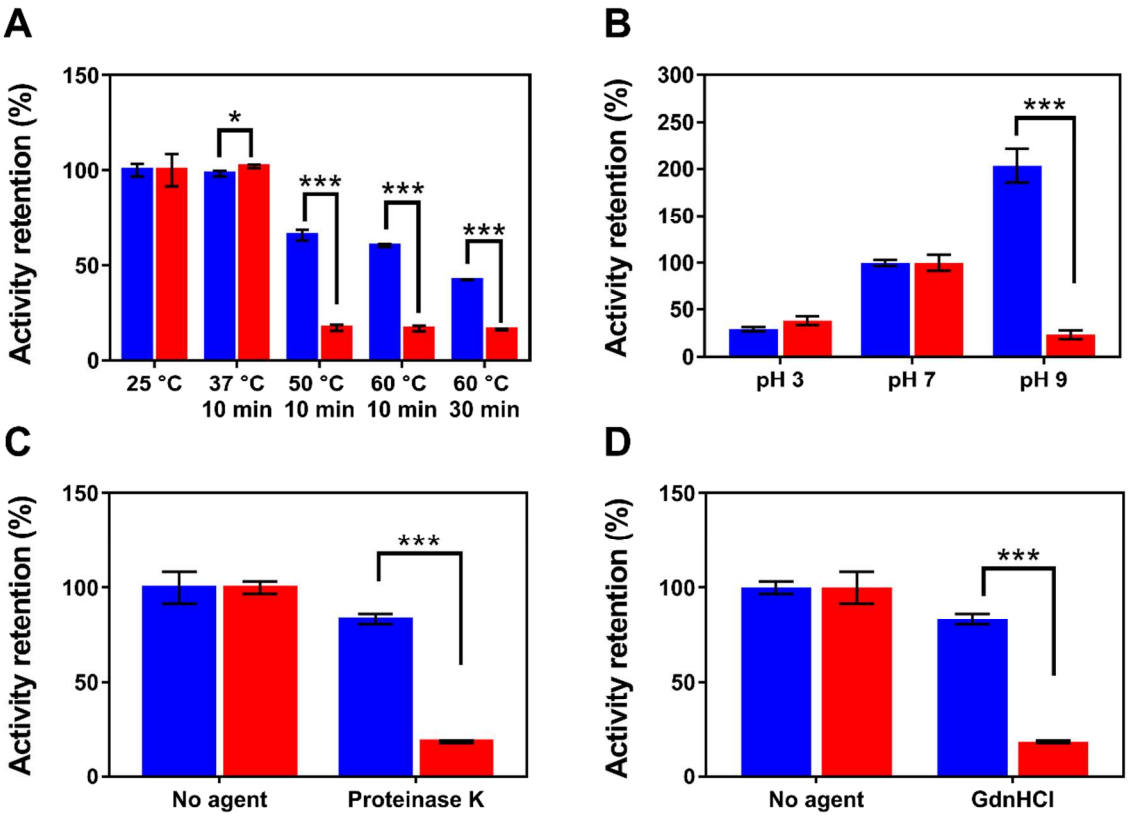

Figure 4. *Stability of catalytic nanocompartments and free enzymes (activity normalized* against *CNCs (blue) or enzymes (red) at RT, neutral pH, no agents).* ***A****: protection from heat.* ***B****: protection from extreme pH.* ***C****: protection from denaturing agent GdnHCl.* ***D****: protection from proteolysis. Error bars are given as mean ± SD (multiple t - test, * $p < 0.05$, ** $p < 0.01$, *** $p < 0.001$, $n = 3$).*

The effect of distance on the efficiency of the CNCs in tandem

The passage through barriers and diffusion between compartments represents an essential point in bio-communication because products have, in some cases, to travel to different cellular compartments or take part in inter-cellular communication. Most organelle-to-organelle

communications in the cell happen via close association below 50 nm[55] and the average synaptic cleft is around 20 nm,[56] whereas it is estimated that a single cell can effectively communicate between 5 and 10 μm in autocrine signaling and up to 250 μm in paracrine signaling.[57-58] In such cases of communication between organelles or cells, there is no longer a homogeneous distribution of enzymes or receptors but local high concentrations and otherwise empty or low density interstices. We used our CNCs in tandem to mimic communication between bio-assemblies and see the effect of distance on the overall cascade reaction efficiency. We assumed a cubic volume for the compartments, so that the mean inter-compartment distance is calculated, based on the polymersome density obtained by FCS.

The AR conversion values in the case of CNCs in tandem remains almost constant (with some values higher than 100% as values fluctuate around the mean obtained at 0.8 μm, set as reference) until the mean distance between CNCs is 1.3 μm, then the values decrease significantly. This suggests that the diffusion of molecules through the OmpF pores represents the dominant factor for distances lower than approximately 1.30 μm. Interestingly, the ratio between the mean inter-compartment distance and their diameter is about 10, which has the same order of magnitude as the ratio between a mean cell-cell communication distance for cells with a 1 μm diameter, such as bacteria.[59] For distances between CNCs higher than 1.3 μm, the cascade reaction is rapidly hindered due to a decrease in the probability that H_2O_2 encounters a HRP-CNC (Figure 5). These distances are consistent with distances typical for autocrine signaling. Therefore our findings, based on tandem CNCs in a simplified medium, represents a first necessary step for better understanding cell communication.

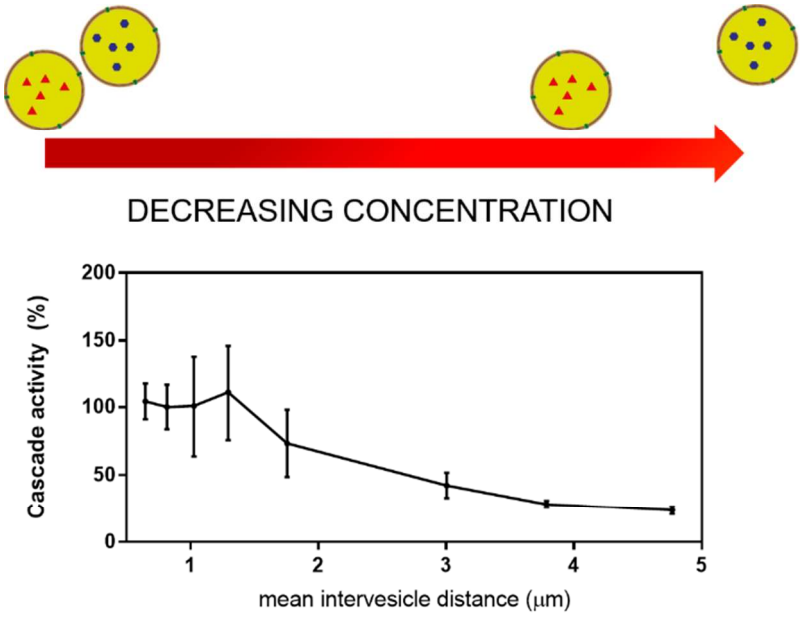

***Figure 5**. AR conversion by cascade reaction inside CNCs in tandem at different mean inter-vesicle distances. Error bars are given as mean ± SD (n = 3).*

CNCs in tandem in biologic conditions

We then evaluated the functionality of the CNCs in biological conditions, both in biofluids and upon incubation with cells, as more apropriate to advance translational applications. First, we used human blood serum where uric acid was dissolved to reach levels similar to those considered typical for hyperucemia (>6.8 mg dL^{-1} in men[60]). A simple model, defined as $\frac{\frac{\Delta Abs290_{with\ enzyme}}{min}}{\frac{\Delta Abs290_{no\ enzyme}}{min}}$ for the dilutions of HRP-CNCs, gives the relative efficiency of the cascade reaction, which we called Relative Urate Degradation (R.U.D.) (Figure 6A). Interestingly, in such a complex medium, CNCs facilitate the clearance of uric acid at a comparable rate to the free enzyme. The addition of HRP removes H_2O_2, pulling the first reaction forward according to Le Chatelier's principle. In addition, we observed no aggregation of polymersomes in serum, in agreement with reported results on similar polymers.[61] Note that only in PBS the free enzymes

are better in terms of the cascade efficiency than when encapsulated inside polymersomes. However, in serum, they perform similarly, which emphasizes the role of the compartments in protecting the encapsulated enzymes in these conditions (37 °C, 6 hours), and support our approach for further cell assessment. Further studies, beyond the scope of the present one, are necessary to understand the bio-molecular factors affecting the efficiency of the overall cascade reaction between CNCs in human serum.

Second, we determined the ability of the CNCs to metabolize uric acid and degrade H_2O_2 upon incubation with cells, as an essential step towards medical applications. First, we evaluated the cytotoxicity of CNCs when incubated with HEK293T cells overnight at different concentrations of the CNCs (measured in polymer concentration) by MTS assay. CNCs have no cytotoxic effect towards the cells, even at the highest polymer concentration (0.19 μg mL^{-1}) (Figure 6B). Next, CNCs were incubated with HEK293T epithelial cells for 24 h in the presence of increasing amounts of uric acid (250 and 350 μM): at physiological concentration and at the lower end of hyperuricemia values. CNCs, known to be eventually internalized by cells,[7] were added together with uric acid because it accumulates extracellularly to toxic levels: in this manner CNCs directly protect cells by degrading uric acid. Cell viability decreased to around 60% in the presence of 250 μM uric acid. By addition of either free enzymes or the CNCs, the cell viability was unaffected by the presence of uric acid. Increasing the amount of uric acid to 350 μM reduces the viability of the cells to 2%, while the cascade reaction of the free enzymes and of the CNCs in tandem induce a protective effect against uric acid. In addition, due to the combination of enzymes, H_2O_2 is also degraded as a result of the succesful cascade reaction process (Figure 6C and D).

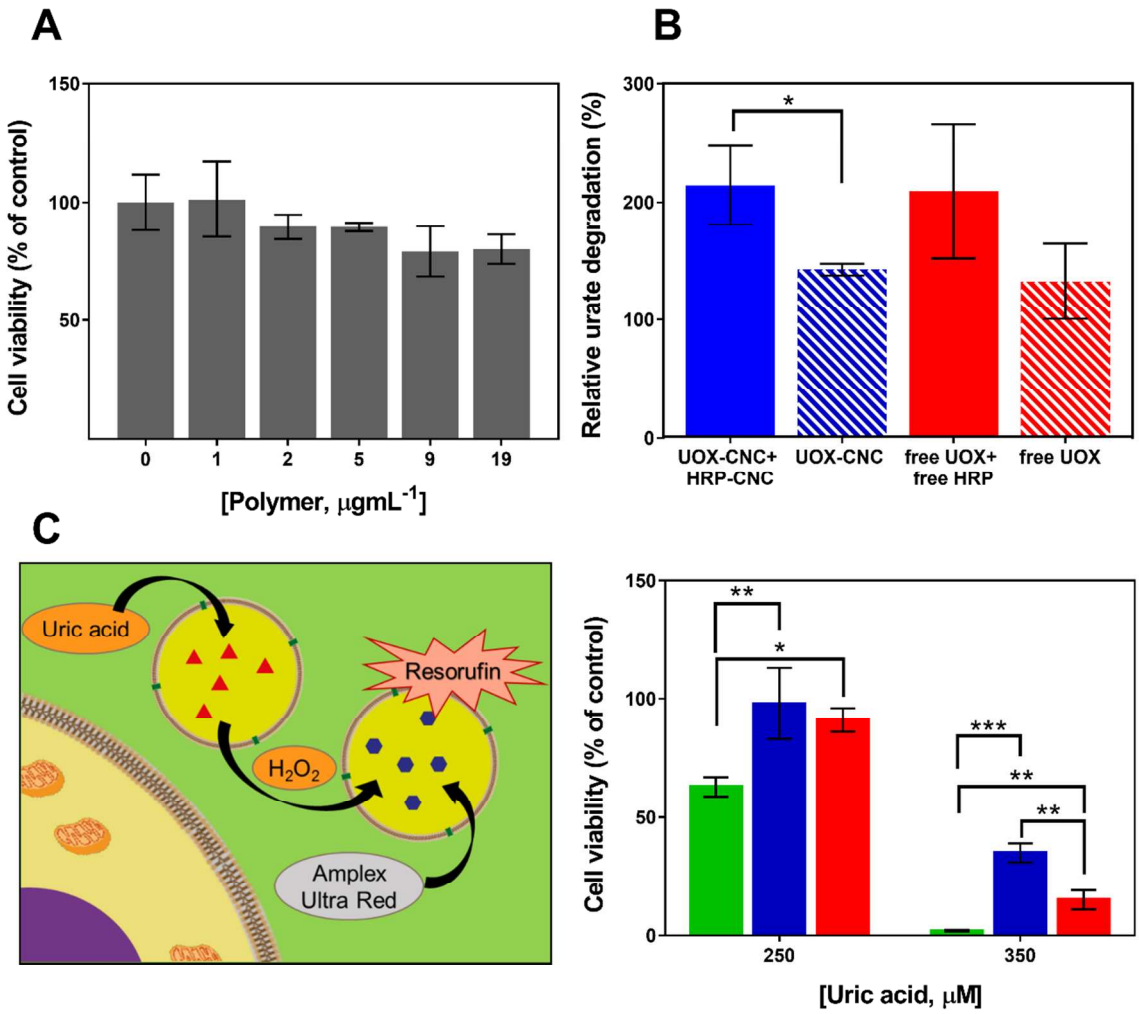

*Figure 6. Activity of CNCs and free enzymes in blood serum and their interaction with cells. **A**: clearance of urate with both CNCs (solid blue), UOX-CNC only (striped blue, no HRP-CNC), both free enzymes (solid red) and UOX only (striped red, no HRP-CNC) **B**: cell viability of HEK293T cells incubated with CNCs at different concentrations (expressed as polymer concentration). **C:** scheme of the CNC-cell interaction and detoxifying activity of the UOX-HRP cascade on cells only (green), cells with free enzymes (blue) and cells with CNCs (red). Error bars are given as mean ± SD (multiple t - test, * $p < 0.05$, ** $p < 0.01$, *** $p < 0.001$, $n = 3$).*

Conclusions

We designed two spatially segregated catalytic nanocompartments to support a cascade reaction between them, mimicking sequential reactions between biosystems. By an elegant selection of

the enzyme combination, we applied these catalytic nanocompartments in tandem to decrease uric acid and H_2O_2, both involved in various pathologic conditions ranging from gout to oxidative stress. A thorough analysis of the factors affecting the overall efficiency of the cascade reaction between CNCs indicated the protective role of the compartments, which provide a shield for the encapsulated enzymes, especially important in biological fluids and cellular environment. For the first time, a kinetic evaluation of a cascade reaction between segregated reaction spaces at the nanoscale has been achieved. We elucidated the limiting factors for the overall reaction: i) the diffusion through the membrane pores inserted into the walls of the compartments and ii) the probability of the products from the first reaction to encounter CNCs containing the second enzyme and reach the encapsulated enzyme molecules. A balance is necessary between the protective role of the nanocompartments and the factors that decrease the efficiency of the cascade reaction for translational applications. This cascade reaction in separate compartments has been successfully performed in serum and then used to decrease both uric acid and the derived H_2O_2 from the cellular milieu as a first step towards medical applications. Our study is the first one that proves that a two-compartment cascade reaction acts in cellular conditions, thus contributing to the understanding of the design of complex catalytic compartments to cope with biological requirements.

Supporting Information

Supporting information: additional physical characterization, enzymatic assays in various conditions, Michaelis-Menten curves. (PDF)

Corresponding Author

Prof. Dr. Cornelia G. Palivan, Department of Chemistry, Physical Chemistry, Mattenstrasse 24a, CH-4058 Basel

cornelia.Palivan@unibas.ch

Author Contributions

A.B contributed to the CNCs production and characterization, I.C contributed to the *in vitro* assays, J.L. contributed to experiment design and enzymatic assays, and C.G.P contributed to the concept of CNCs in tandem. The manuscript was written through contributions of all authors. All authors have given approval to the final version of the manuscript.

Acknowledgements

We gratefully acknowledge the financial support provided by the Swiss National Science Foundation, the University of Basel and the National Centre of Competence in Research – Molecular Systems Engineering. Authors thank Prof. Wolfgang Meier (University of Basel) for providing the polymer, Dr. Samuel Lörcher for its synthesis and Gabriele Persy for the TEM measurements. A.B. thanks Dr. Tomaž Einfalt (University of Basel) for the fruitful help and discussions on handling of OmpF, and Prof. Lucio Isa (ETHZ), for his suggestion regarding the distance mode. Authors thank Federica Rasa for the help with the illustrations.

REFERENCES

1. Kuchler, A.; Yoshimoto, M.; Luginbuhl, S.; Mavelli, F.; Walde, P., Enzymatic reactions in confined environments. *Nat Nanotechnol* **2016,** *11* (5), 409-20.
2. Agapakis, C. M.; Boyle, P. M.; Silver, P. A., Natural strategies for the spatial optimization of metabolism in synthetic biology. *Nat Chem Biol* **2012,** *8* (6), 527-35.
3. Hosta-Rigau, L.; York-Duran, M. J.; Zhang, Y.; Goldie, K. N.; Stadler, B., Confined multiple enzymatic (cascade) reactions within poly(dopamine)-based capsosomes. *ACS Appl Mater Interfaces* **2014,** *6* (15), 12771-9.

4. Sakr, O. S.; Borchard, G., Encapsulation of Enzymes in Layer-by-Layer (LbL) Structures: Latest Advances and Applications. *Biomacromolecules* **2013,** *14* (7), 2117-2135.
5. Palivan, C. G.; Fischer-Onaca, O.; Delcea, M.; Itel, F.; Meier, W., Protein-polymer nanoreactors for medical applications. *Chem Soc Rev* **2012,** *41* (7), 2800-23.
6. Schoonen, L.; van Hest, J. C., Compartmentalization Approaches in Soft Matter Science: From Nanoreactor Development to Organelle Mimics. *Adv Mater* **2016,** *28* (6), 1109-28.
7. Tanner, P.; Onaca, O.; Balasubramanian, V.; Meier, W.; Palivan, C. G., Enzymatic cascade reactions inside polymeric nanocontainers: a means to combat oxidative stress. *Chemistry* **2011,** *17* (16), 4552-60.
8. Blackman, L. D.; Varlas, S.; Arno, M. C.; Fayter, A.; Gibson, M. I.; O'Reilly, R. K., Permeable Protein-Loaded Polymersome Cascade Nanoreactors by Polymerization-Induced Self-Assembly. *ACS Macro Lett* **2017,** *6* (11), 1263-1267.
9. Peters, R. J.; Marguet, M.; Marais, S.; Fraaije, M. W.; van Hest, J. C.; Lecommandoux, S., Cascade reactions in multicompartmentalized polymersomes. *Angew Chem Int Ed Engl* **2014,** *53* (1), 146-50.
10. Grafe, D.; Gaitzsch, J.; Appelhans, D.; Voit, B., Cross-linked polymersomes as nanoreactors for controlled and stabilized single and cascade enzymatic reactions. *Nanoscale* **2014,** *6* (18), 10752-61.
11. Taek, K. K.; M., C. J. J. L.; M., N. R. J.; M., v. H. J. C., A Polymersome Nanoreactor with Controllable Permeability Induced by Stimuli-Responsive Block Copolymers. *Advanced Materials* **2009,** *21* (27), 2787-2791.
12. Schmitt, C.; Lippert, A. H.; Bonakdar, N.; Sandoghdar, V.; Voll, L. M., Compartmentalization and Transport in Synthetic Vesicles. *Front Bioeng Biotechnol* **2016,** *4*, 19.
13. Lomora, M.; Garni, M.; Itel, F.; Tanner, P.; Spulber, M.; Palivan, C. G., Polymersomes with engineered ion selective permeability as stimuli-responsive nanocompartments with preserved architecture. *Biomaterials* **2015,** *53* (0), 406-414.
14. van Oers, M. C.; Rutjes, F. P.; van Hest, J. C., Cascade reactions in nanoreactors. *Curr Opin Biotechnol* **2014,** *28*, 10-6.
15. Bolinger, P. Y.; Stamou, D.; Vogel, H., An integrated self-assembled nanofluidic system for controlled biological chemistries. *Angew Chem Int Ed Engl* **2008,** *47* (30), 5544-9.
16. Brasch, M.; Putri, R. M.; de Ruiter, M. V.; Luque, D.; Koay, M. S.; Caston, J. R.; Cornelissen, J. J., Assembling Enzymatic Cascade Pathways inside Virus-Based Nanocages Using Dual-Tasking Nucleic Acid Tags. *J Am Chem Soc* **2017,** *139* (4), 1512-1519.
17. Marguet, M.; Bonduelle, C.; Lecommandoux, S., Multicompartmentalized polymeric systems: towards biomimetic cellular structure and function. *Chem Soc Rev* **2013,** *42* (2), 512-29.
18. Godoy-Gallardo, M.; Labay, C.; Jansman, M. M. T.; Ek, P. K.; Hosta-Rigau, L., Intracellular Microreactors as Artificial Organelles to Conduct Multiple Enzymatic Reactions Simultaneously. *Advanced Healthcare Materials* **2016,** *6* (4), 1601190.
19. Kuiper, S. M.; Nallani, M.; Vriezema, D. M.; Cornelissen, J. J.; van Hest, J. C.; Nolte, R. J.; Rowan, A. E., Enzymes containing porous polymersomes as nano reaction vessels for cascade reactions. *Org Biomol Chem* **2008,** *6* (23), 4315-8.
20. Liu, X.; Formanek, P.; Voit, B.; Appelhans, D., Functional Cellular Mimics for the Spatiotemporal Control of Multiple Enzymatic Cascade Reactions. *Angewandte Chemie International Edition* **2017,** *56* (51), 16233-16238.

21. Wang, Z.; van Oers, M. C. M.; Rutjes, F. P. J. T.; van Hest, J. C. M., Polymersome Colloidosomes for Enzyme Catalysis in a Biphasic System. *Angewandte Chemie* **2012,** *124* (43), 10904-10908.
22. Wertheimer, A.; Morlock, R.; Becker, M. A., A revised estimate of the burden of illness of gout. *Current therapeutic research, clinical and experimental* **2013,** *75*, 1-4.
23. Lörcher, S.; Meier, W., Cosolvent fractionation of PMOXA-b-PDMS-b-PMOXA: Bulk separation of triblocks from multiblocks. *European Polymer Journal* **2017,** *88*, 575-585.
24. Nardin, C.; Thoeni, S.; Widmer, J.; Winterhalter, M.; Meier, W., Nanoreactors based on (polymerized) ABA-triblock copolymer vesicles. *Chemical Communications* **2000,** (15), 1433-1434.
25. Azmi, N. E.; Ramli, N. I.; Abdullah, J.; Abdul Hamid, M. A.; Sidek, H.; Abd Rahman, S.; Ariffin, N.; Yusof, N. A., A simple and sensitive fluorescence based biosensor for the determination of uric acid using H2O2-sensitive quantum dots/dual enzymes. *Biosens Bioelectron* **2015,** *67*, 129-33.
26. Dai, M.; Huang, T.; Chao, L.; Xie, Q.; Tan, Y.; Chen, C.; Meng, W., Horseradish peroxidase-catalyzed polymerization of L-DOPA for mono-/bi-enzyme immobilization and amperometric biosensing of H2O2 and uric acid. *Talanta* **2016,** *149*, 117-123.
27. Miland, E.; Miranda Ordieres, A. J.; Tunon Blanco, P.; Smyth, M. R.; Fagain, C. O., Poly(o-aminophenol)-modified bienzyme carbon paste electrode for the detection of uric acid. *Talanta* **1996,** *43* (5), 785-96.
28. Einfalt, T.; Goers, R.; Dinu, I. A.; Najer, A.; Spulber, M.; Onaca-Fischer, O.; Palivan, C. G., Stimuli-Triggered Activity of Nanoreactors by Biomimetic Engineering Polymer Membranes. *Nano Lett* **2015,** *15* (11), 7596-603.
29. JW. Krieger; Langowski, J. *QuickFit 3.0: A data evaluation application for biophysics*, http://www.dkfz.de/Macromol/quickfit/, 2015.
30. Baumann, P.; Spulber, M.; Fischer, O.; Car, A.; Meier, W., Investigation of Horseradish Peroxidase Kinetics in an "Organelle-Like" Environment. *Small* **2017,** *13* (17).
31. Stauch, O.; Schubert, R., Structure of Artificial Cytoskeleton Containing Liposomes in Aqueous Solution Studied by Static and Dynamic Light Scattering. *Biomacromolecules* **2002**.
32. Habel, J.; Ogbonna, A.; Larsen, N.; Cherre, S.; Kynde, S.; Midtgaard, S. R.; Kinoshita, K.; Krabbe, S.; Jensen, G. V.; Hansen, J. S.; Almdal, K.; Helix-Nielsen, C., Selecting analytical tools for characterization of polymersomes in aqueous solution. *RSC Advances* **2015,** *5* (97), 79924-79946.
33. Edlinger, C.; Einfalt, T.; Spulber, M.; Car, A.; Meier, W.; Palivan, C. G., Biomimetic Strategy To Reversibly Trigger Functionality of Catalytic Nanocompartments by the Insertion of pH-Responsive Biovalves. *Nano Lett* **2017,** *17* (9), 5790-5798.
34. Chen, Q.; Schönherr, H.; Vancso, G. J., Block-Copolymer Vesicles as Nanoreactors for Enzymatic Reactions. *Small* **2009,** *5* (12), 1436-1445.
35. Bar-Even, A.; Noor, E.; Savir, Y.; Liebermeister, W.; Davidi, D.; Tawfik, D. S.; Milo, R., The moderately efficient enzyme: evolutionary and physicochemical trends shaping enzyme parameters. *Biochemistry* **2011,** *50* (21), 4402-10.
36. Garcia-Viloca, M.; Gao, J.; Karplus, M.; Truhlar, D. G., How enzymes work: analysis by modern rate theory and computer simulations. *Science* **2004,** *303* (5655), 186-95.
37. Caliceti, P.; Schiavon, O.; Veronese, F. M., Biopharmaceutical properties of uricase conjugated to neutral and amphiphilic polymers. *Bioconjug Chem* **1999,** *10* (4), 638-46.

38. Rennke, H. G.; Patel, Y.; Venkatachalam, M. A., Glomerular filtration of proteins: clearance of anionic, neutral, and cationic horseradish peroxidase in the rat. *Kidney Int* **1978,** *13* (4), 278-88.
39. Itel, F.; Chami, M.; Najer, A.; Lörcher, S.; Wu, D.; Dinu, I. A.; Meier, W., Molecular Organization and Dynamics in Polymersome Membranes: A Lateral Diffusion Study. *Macromolecules* **2014,** *47* (21), 7588-7596.
40. Cao, X.; Chen, C.; Yu, H.; Wang, P., Horseradish peroxidase-encapsulated chitosan nanoparticles for enzyme-prodrug cancer therapy. *Biotechnology letters* **2015,** *37* (1), 81-8.
41. Ihle, S.; Onaca, O.; Rigler, P.; Hauer, B.; Rodríguez-Ropero, F.; Fioroni, M.; Schwaneberg, U., Nanocompartments with a pH release system based on an engineered OmpF channel protein. *Soft Matter* **2011,** *7* (2), 532-539.
42. Nestorovich, E. M.; Rostovtseva, T. K.; Bezrukov, S. M., Residue Ionization and Ion Transport through OmpF Channels. *Biophysical Journal* **2003,** *85* (6), 3718-3729.
43. Phale, P. S.; Philippsen, A.; Kiefhaber, T.; Koebnik, R.; Phale, V. P.; Schirmer, T.; Rosenbusch, J. P., Stability of trimeric OmpF porin: the contributions of the latching loop L2. *Biochemistry* **1998,** *37* (45), 15663-70.
44. Mukherjee, S.; Guptasarma, P., Direct proteolysis-based purification of an overexpressed hyperthermophile protein from Escherichia coli lysate: a novel exploitation of the link between structural stability and proteolytic resistance. *Protein Expression and Purification* **2005,** *40* (1), 71-76.
45. Yan, M.; Ge, J.; Liu, Z.; Ouyang, P., Encapsulation of Single Enzyme in Nanogel with Enhanced Biocatalytic Activity and Stability. *Journal of the American Chemical Society* **2006,** *128* (34), 11008-11009.
46. Cecchin, D.; Battaglia, G. In *Protein stabilisation by polymersome entrapment*, **2016**.
47. Critchlow, J. E.; Dunford, H. B., Studies on Horseradish Peroxidase *The Journal of Biological Chemistry* **1972**.
48. Mahler, H. R. a.; Baum, H. M. c.; Hübscher, G., Enzymatic oxidation of urate. *Science* **1956**.
49. Moosavi-Movahedi, A. A.; Nazari, K.; Saboury, A. A., Thermodynamics of denaturation of horseradish peroxidase with sodium n-dodecyl sulphate and n-dodecyl trimethylammonium bromide. *Colloids and Surfaces B: Biointerfaces* **1997,** *9* (3), 123-130.
50. Di Risio, S.; Yan, N., Adsorption and inactivation behavior of horseradish peroxidase on cellulosic fiber surfaces. *J Colloid Interface Sci* **2009,** *338* (2), 410-419.
51. Saint, N.; Lou, K. L.; Widmer, C.; Luckey, M.; Schirmer, T.; Rosenbusch, J. P., Structural and functional characterization of OmpF porin mutants selected for larger pore size. II. Functional characterization. *J Biol Chem* **1996,** *271* (34), 20676-80.
52. Rosenkranz, T.; Katranidis , A.; Atta, D.; Gregor , I.; Enderlein, J.; Grzelakowski, M.; Rigler, P.; Meier, W.; Fitter, J., Observing Proteins as Single Molecules Encapsulated in Surface-Tethered Polymeric Nanocontainers. *ChemBioChem* **2009,** *10* (4), 702-709.
53. Pitts, O. M.; Priest, D. G.; Fish, W. W., Uricase. Subunit composition and resistance to denaturants. *Biochemistry* **1974,** *13* (5), 888-92.
54. Pace, C. N.; Hermans, J., The Stability of Globular Protein. *CRC Critical Reviews in Biochemistry* **1975,** *3* (1), 1-43.
55. Achleitner, G.; Gaigg, B.; Krasser, A.; Kainersdorfer, E.; Kohlwein, S. D.; Perktold, A.; Zellnig, G.; Daum, G., Association between the endoplasmic reticulum and mitochondria of

yeast facilitates interorganelle transport of phospholipids through membrane contact. *Eur J Biochem* **1999,** *264* (2), 545-53.
56. Barberis, A.; Petrini, E. M.; Mozrzymas, J. W., Impact of synaptic neurotransmitter concentration time course on the kinetics and pharmacological modulation of inhibitory synaptic currents. *Front Cell Neurosci* **2011,** *5*, 6.
57. Francis, K.; Palsson, B. O., Effective intercellular communication distances are determined by the relative time constants for cyto/chemokine secretion and diffusion. *Proc Natl Acad Sci U S A* **1997,** *94* (23), 12258-62.
58. Shvartsman, S. Y.; Wiley, H. S.; Deen, W. M.; Lauffenburger, D. A., Spatial range of autocrine signaling: modeling and computational analysis. *Biophys J* **2001,** *81* (4), 1854-67.
59. Chien, A. C.; Hill, N. S.; Levin, P. A., Cell size control in bacteria. *Curr Biol* **2012,** *22* (9), R340-9.
60. Maiuolo, J.; Oppedisano, F.; Gratteri, S.; Muscoli, C.; Mollace, V., Regulation of uric acid metabolism and excretion. *Int J Cardiol* **2016,** *213*, 8-14.
61. Murdoch, C.; Reeves, K. J.; Hearnden, V.; Colley, H.; Massignani, M.; Canton, I.; Madsen, J.; Blanazs, A.; Armes, S. P.; Lewis, A. L.; Macneil, S.; Brown, N. J.; Thornhill, M. H.; Battaglia, G., Internalization and biodistribution of polymersomes into oral squamous cell carcinoma cells in vitro and in vivo. *Nanomedicine* **2010,** *5* (7), 1025-36.